This is an *Accepted Manuscript*, which has been through the Royal Society of Chemistry peer review process and has been accepted for publication.

Accepted Manuscripts are published online shortly after acceptance, before technical editing, formatting and proof reading. Using this free service, authors can make their results available to the community, in citable form, before we publish the edited article. We will replace this *Accepted Manuscript* with the edited and formatted *Advance Article* as soon as it is available.

You can find more information about *Accepted Manuscripts* in the **Information for Authors**.

Please note that technical editing may introduce minor changes to the text and/or graphics, which may alter content. The journal's standard **Terms & Conditions** and the **Ethical guidelines** still apply. In no event shall the Royal Society of Chemistry be held responsible for any errors or omissions in this *Accepted Manuscript* or any consequences arising from the use of any information it contains.

Journal Name

ARTICLE

Size-Selective, Biocompatible, Manufacturable Platform for Structuring Deformable Microsystems

Gunjan Agarwal,[a] Amelia Servi[b] and Carol Livermore[c]

Precise, size-selective assembly and sorting are demonstrated in a low-cost system using manufacturable, replicated polymer templates to guide the assembly. Surface interactions between microscale objects and an assembly template are combined with fluid forces to drive site-selective organization of objects onto the template. Although controlling the organization of deformable objects on deformable surfaces offers a key tool for biological applications, the deformability can potentially interfere with the process that drives size selectivity. Theoretical models of the polymer assembly system were created to predict when selectivity will fail in deformable systems and were validated by comparison with experiments. Selective template-driven assembly of polystyrene microspheres on PDMS templates replicated from silicon masters was carried out using templated assembly by selective removal (TASR), demonstrating the effectiveness of selective assembly with low-cost, manufacturable materials and processes. The assembly of polystyrene microcomponents on PDMS shows high assembly yields and effective selectivity, in agreement with models.

Introduction

Systems for structuring or analyzing biological specimens face competing requirements. On one hand, the need for low cost processes and devices drives the use of polymer replication and patterning techniques [1-2]. A great many polymer-based systems have been demonstrated for applications from tissue engineering [3], to biochemical assays [4], to chip-based cell growth monitoring systems [5]. On the other hand, many such applications require precision in the location and placement of individual microcomponents or cells. Precision placement must be engineered into systems and can often require greater tool and process expense. For example, bio-printing can control the 3D organization of cells [6], but it is accomplished by equipment that drives top-down organization through a serial process. At the other extreme, cells and microcomponents can be passively organized into predefined 2D arrangements on precisely-controlled, micro- or nanostructured, rigid templates under the guiding influence of the template's topography [7-11]. However, the template's structure is implemented in a conventionally-microfabricated, silicon-based system that is not compatible with low-cost applications.

A range of techniques that make use of a wide variety of forces to trap or sort individual components have been implemented in efforts to bridge this gap between precision and low cost [12-18]. For example, techniques that use dielectrophoretic trapping [19], optical tweezers [20], electrophoretic microwells [21], surface chemistry [22], mechanical trapping [23] and microfluidic trapping [24] have been employed to sort and position microcomponents. However, all of these techniques suffer from drawbacks involving limited selectivity (e.g. microfluidic and mechanical trapping techniques), elaborate set up (e.g. optical methods), or the risk of specimen damage (e.g. dielectrophoresis or electrophoretic microwells). In other examples, controlling the interactions among colloidal micro-particles can create a wide range of periodic or quasi-periodic patterns [25-27], but these methods do not inherently offer control of the microcomponents' positions relative to the target substrate.

The present work bridges the gap between precise control of the assembled structure and the use of low-cost, polymer materials and replication processes by demonstrating the highly selective assembly of model components (polystyrene microspheres) onto polydimethylsiloxane (PDMS) templates replicated from a well-controlled silicon master. This material system is chosen because the components represent one of the worst-case scenarios for size-selective assembly of mechanically deformable objects, and because of the extensive application of PDMS in practical systems. The present research organizes the components using templated assembly by selective removal (TASR), which locates components into shape- and size-matched wells in a template's surface [7-11]. This approach leverages interactions (e.g. hydrophobic interactions or cell adhesion) between the components and substrate to promote assembly of the components on the surface. These interactions are strongest where the shapes and sizes of the components match the shapes and sizes of the wells. Selectivity is achieved when fluid forces created by externally-input, high frequency (MHz-range) acoustic excitations dislodge components from any poorly-matched wells in which they may have assembled. Quasi-random assembly and deterministic selective removal proceed until the

system is nearly fully assembled. This technique is particularly well matched to systems at biological and optical length scales.

Although the TASR concept has previously been demonstrated to achieve highly selective organization of inorganic micro-components and biological cells [7-11] on patterned rigid substrates, its use with economical, replicated polymer templates has not previously been demonstrated or modeled. The inclusion of deformable materials in the assembly system has been considered, but only in the context of deformable components. Models created to explain the selective assembly of rigid components on rigid substrates [7-9] were extended in [10,11] to describe some cases of interaction between deformable components or biological cells and rigid substrates. However, in all previous work, assembly templates were rigid and were fabricated by conventional, top-down, silicon-based micromachining. The previously neglected case of assembly onto deformable polymer templates is nonetheless of practical importance and scientific interest. Polymer templates offer a particular challenge for this type of assembly; the key element of shape for shape- and size-matching is questionable for systems in which the shape of the polymer template changes under applied loads. This work demonstrates for the first time the effectiveness of the TASR process for selectively organizing deformable microscale objects onto replicated polymer templates. It also presents theoretical models that can predict the success or failure of assembly in this and other material systems.

Theoretical Model

The original TASR theory explains the selective self-assembly process as a combination of essentially random assembly and deterministic selective removal [7-9]. According to this theory, which describes the interaction of rigid objects, whether a component can be assembled in a given assembly site (a given well) on the substrate is effectively predicted by whether the mechanical moments (caused by adhesion) that oppose removal of the component from the well are larger than the mechanical moments (caused by the acoustic fluid excitation) that promote removal by rolling the component out of the well. Since deformable structures can change in shape and size under the application of a load, the component/template contact area and interaction strength for deformable structures depend on the degree of deformation. The TASR theory must therefore be adapted to predict the effects of deformability on assembly selectivity.

The models of TASR-based assembly for rigid systems describe a process of energy minimization in which sufficiently large mechanical moments are required to drive the system over an energy barrier and into a new configuration. The degree of shape matching dictates the energy landscape and determines the magnitudes of its resulting conservative forces. It is proposed here and in [10] that the key requirement for TASR to work with deformable structures is that the deformations should be fully elastic, so that the reduction in energy from increasing the area of contact is offset by the increase in elastic energy. As long as this holds true, the original TASR model will provide accurate predictions of assembly in deformable systems. If, however, the applied forces result in plastic deformation of either the components or the substrate, the predictions of the original TASR model will become invalid and the assembly may at best be marginally successful.

The effects of component deformability on assembly onto a rigid substrate were modeled and verified experimentally in

[10]. The attractive force between the component and the substrate produces a deformation in the component, which is determined by quantifying the contact mechanism. However, it is also important to consider the effects of template deformability. For example, if biological cells are assembled onto a scaffold for tissue engineering, the scaffold will likely be made of a biodegradable polymer such as poly (glycerol sebacate) (PGS). If cells are assembled onto a template for a cell sorting application, the template will likely be made of similarly deformable PDMS. Although TASR's effectiveness for cell assembly onto rigid substrates is demonstrated in [11], its use with these types of deformable substrates has not been previously addressed. Similarly, biosensors that utilize functionalized microspheres may be economically assembled onto PDMS, but TASR-based assembly for this case has also not been previously studied.

A model is presented here that accounts for both template deformation and component deformation for cases of assembly involving polymers, biomaterials, and biological cells. Although this model applies specifically to the common case of spherical components, the model can be readily extended to components having other geometries (e.g. cylinders) by incorporating different radii of curvature in different directions into the equations below.

The case of a component made from a relatively rigid material contacting a deformable substrate is considered first. Based on the case of Brinnel indentation of an elastic-plastic half-space by a rigid sphere [28], the parameter γ that describes the nature of deformation in the substrate is defined as

$$\gamma = \frac{E'a}{R_{eq}\sigma_o} \, . \tag{1}$$

The parameter γ is the ratio of the indentation pressure (given by $E'a/R_{eq}$) to the initial yield strength σ_o of the half-space, in this case the assembly site on the substrate. Here R_{eq} is the equivalent radius of curvature that takes into account the radii of curvature of both the assembly component R_c and the hemispherical well on the assembly template R_t. The equivalent radius is given by

$$\frac{1}{R_{eq}} = \frac{1}{R_c} + \frac{1}{R_t} \, . \tag{2}$$

E' is the combined modulus of the component and template materials, given by

$$\frac{1}{E'} = \frac{(1-\upsilon_c^2)}{E_c} + \frac{(1-\upsilon_t^2)}{E_t} \, , \tag{3}$$

and a is the radius of the circular contact area, given by

$$A = \pi a^2 = \pi \left(\frac{3R_{eq}F}{4E'} \right)^{2/3} \, . \tag{4}$$

The quantity F is the contact load applied on the sphere, and it is typically dominated by the interaction force that attracts the component to the assembly site well.

The mechanical behavior of the deformable materials is described using an elastic-perfectly plastic model. The elastic-plastic model is suitable to describe the mechanical behavior of polymers such as PMMA, polystyrene, polypropylene, etc. under the conditions imposed by the TASR setup. While some commonly used rubber-like polymers (e.g. PDMS, PGS) exhibit non-linear behavior at large deformation values, for the smaller deformations considered here, their behavior is in the short linear range. Therefore, the Hertzian contact theory used to describe other polymers that are idealized as exhibiting

TABLE 1

Mechanical deformation assessment for interaction of different substrate materials with a 2 µm diameter silica microsphere.

Substrate material	γ value on indentation
Teflon (PTFE)	1.22
PMMA	0.75
Polystyrene (PS)	3.05
Polypropylene	0.95
Melamine	1.61
PDMS	0.03
poly(glycerol sebacate) (PGS)	0.68
Polycaprolactone (PCL)	1.01
poly(sorbitol sebacate) (PSS)	0.15
poly(maltitol sebacate) (PMtS)	0.53

TABLE 2

Mechanical deformation assessment for contact between 2 µm diameter spherical components made of different deformable materials and PDMS and PGS substrates.

Component material	ω/ω_c value on PDMS	ω/ω_c value on PGS
Teflon (PTFE)	2.43E-05	2.75E-05
PMMA	2.04E-06	2.32E-06
Polystyrene (PS)	4.08E-05	4.33E-05
Polypropylene	2.13E-06	2.41E-06
Melamine	7.77E-07	8.83E-07
PDMS	1.48E-05	2.28E-05
poly(glycerol sebacate) (PGS)	1.50E-02	2.84E-02
Polycaprolactone (PCL)	2.75E-05	7.95E-05
poly(sorbitol sebacate) (PSS)	1.49E-03	2.19E-03
poly(maltitol sebacate) (PMtS)	6.16E-06	1.78E-05
Lung carcinoma cells	5.19E-06	6.27E-06
Human embryonic stem cells (hESCs)	1.10E-05	1.26E-05

elastic-perfectly plastic behavior is extended to encompass behavior of rubbery materials within the range of deformations experienced in TASR assembly.

From finite element predictions [28] of average indentation pressure, the completely elastic Hertzian regime extends for values of γ less than 2.5. Above this value, plastic deformation begins in the substrate. Table 1 lists values of the ratio γ for the interaction of various polymer-based substrate materials with relatively rigid silica microspheres that are 2 µm in diameter. For the purposes of these calculations, the force is assumed to have a magnitude of 4.05 nN, corresponding to a typical hydrophobic interaction between a 2 µm diameter assembly component and a flat template surface. The contact is predicted to be purely elastic for all but one of the substrate materials examined here, including bio-compatible polymers such as PGS and polycaprolactone (PCL). The value of γ is seen to exceed the critical limit for polystyrene substrates, which are less common in biological applications. In the case of polystyrene (PS), the resulting shape change due to plastic deformation may lead to unsuccessful or marginally successful assembly. For constant contact load and geometry, this represents an upper bound on substrate deformation; the substrate deformation arising from a deformable component will be less than that arising from a rigid component. Due to its low ratio of stiffness to strength, contact on PDMS substrates results in the lowest value of the ratio γ among the materials considered. PDMS therefore is predicted to remain entirely in the elastic regime.

For assembly of polymers or cells, the objects being assembled are typically also highly deformable. The concepts of Hertzian theory are combined with the above analysis of plastic deformation of a deformable substrate by a rigid sphere. The resulting model describes deformations during assembly of deformable microspheres on deformable substrates. First the possibility of plastic deformation in the deformable substrate material is investigated upon interaction with a more rigid component material. If the substrate doesn't deform plastically, then it may safely be assumed to have elastic behavior on contact with more deformable materials under otherwise similar circumstances. The next step is to consider the possibility of deformation of the component by the substrate. Component deformation is captured by the model of [10], which quantifies a sphere's deformation in terms of the interference ω. The interference describes the amount by which the distance from the center of a sphere to the underlying surface is less than the radius of the undeformed sphere. The interference is calculated for the given set of mechanical properties and is compared to

the critical interference value ω_c [29-30] that marks the transition from the purely elastic to the elastic–plastic deformation regime.

Table 2 shows values of the ω/ω_c ratio for a range of representative components assembled onto PDMS and PGS substrates. The assembled components range from polymers to biological cells. The effective mechanical properties of different types of cells span a wide range, with elastic moduli anywhere from a few kPa to tens of MPa. The mechanical properties of only a few mammalian cell types (lung carcinoma cells and human embryonic stem cells with elastic moduli of 150 KPa and 25 KPa, respectively) were considered here to assess the possibility of implementing assembled biological systems, such as engineered tissue or cell sorting platforms. The results show that all of the material combinations considered here may be expected to remain in the elastic regime at the few micron size scale under the influence of nN-scale attractive forces, with some biopolymers (e.g. PGS) approaching the onset of plastic deformation more closely than is predicted for the other materials considered here. These models may be combined with the original TASR model for rigid components and templates to predict geometries and material combinations that can be successfully and selectively assembled.

Experiments

The TASR-based assembly of polystyrene (PS) microspheres on PDMS templates was examined experimentally and compared with model predictions. Polystyrene is chosen because (i) it shows a relatively early onset of plastic deformation, (ii) it is relevant to biosensors, and (iii) its predicted values for ω/ω_c are similar to those of some biological cells. PDMS templates are chosen for their extremely high relevance to biological applications.

Template Fabrication

Assembly templates were fabricated by replicating silicon-based master patterns in PDMS. In addition to creating deformable templates with which to test the models, this
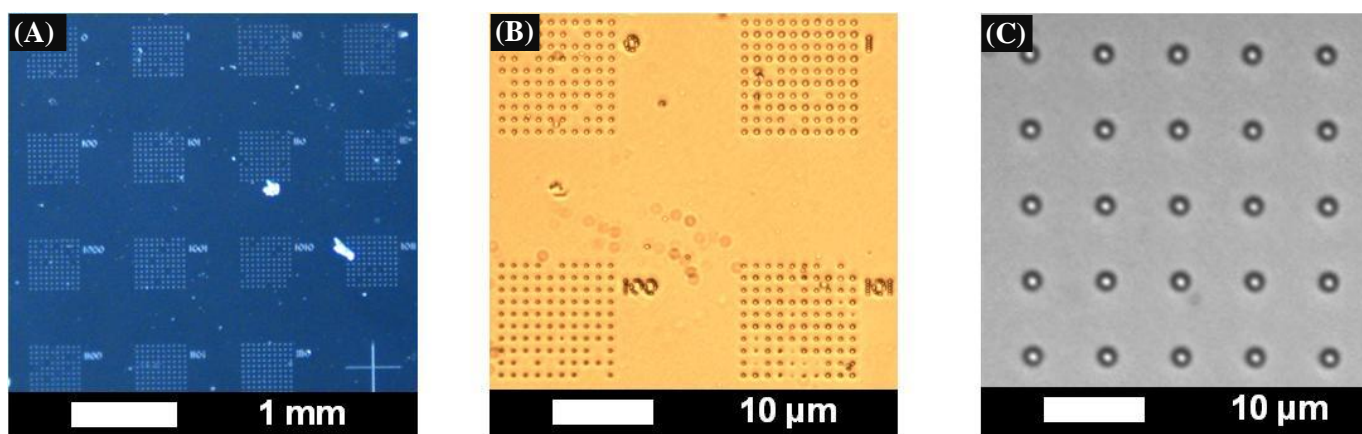
Fig. 1: Optical micrographs of the deformable PDMS templates replicated from the silicon master. (A) Overview of a PDMS chip showing several arrays containing wells with resist openings of different sizes. (B) Zoomed-in view of arrays on the chip. (C) An array of nominally uniform assembly wells.

approach greatly reduces the cost of template manufacture. Top down manufacturing of templates that contain nearly hemispherical wells to drive the size-selective organization of microspherical components is cost prohibitive. For example, the nearly hemispherical wells at the few micron scale in the master patterns used here were created using electron beam (e-beam) lithography followed by an isotropic etch. Details of the process sequence to create PDMS templates are described below.

Fabrication of the master template is as described in [10]. A silicon wafer was oxidized to form a 1.7 μm thick layer of silicon dioxide. An e-beam resist (PMMA) was patterned by e-beam lithography to create openings in the resist with diameters ranging from 45-75 nm. The oxide was etched in BOE to a depth of approximately 1 μm to create nearly hemispherical wells around the resist openings. Deformable PDMS replicas were then created from the master silicon templates. The master templates were silanized by placing them in a vacuum chamber along with three drops of HDMS on a glass slide for one hour; the resulting hydrophobic surface reduces adhesion between the template and the PDMS. A 10:1 mixture by weight of PDMS pre-polymer with its curing agent (Sylgard 184 elastomer from Dow Corning) was degassed in vacuum for 10-15 minutes, poured onto the wafer to a thickness of about 6 mm, cured at 130°C for 20 minutes, and peeled off the wafer to form an inverse replica. To create replicas in the same tone as the original template, the first PDMS copy was replicated using a similar process as above. Unlike the original mold process, the PDMS copy was not silanized, following a procedure similar to that used in [31-32]. After curing, the PDMS layers were peeled apart gently with a razor blade.

Figure 1 shows optical micrographs of the PDMS replicas made from the silica templates. The resulting wells on the substrate are about 1 μm deep, quasi-hemispherical holes that match (to varying degrees) the 2 μm diameter polystyrene microspheres to be assembled. The finite sizes of the initial resist openings result in etched wells that deviate slightly from the ideal hemispherical shape; the larger the resist opening, the larger the deviation. This is evident in Figure 2, which shows AFM profiles of quasi-hemispherical wells etched from resist openings of various sizes.

Experimental Procedure

The experimental apparatus is similar to that described in [10]. To generate acoustic excitation, an acoustic transducer at a frequency of 1.7 MHz was placed at the bottom of a large (1325 cc) beaker filled with water, with the height of water above the transducer kept at 4 cm. The high transducer frequency ensured that the operating point was below the intensity threshold for fully-developed cavitation. A variable voltage transformer controlled the input voltage to the transducer over the range from 20 V to 60 V.

Deep-blue dyed polystyrene microspheres, with a diameter of 2.004 (± 0.08) μm, were purchased dispersed in water from Phosphorex, Inc. (catalog no. 1002KB). The color offers high contrast to the transparent PDMS polymer surface for improved visibility during optical imaging. The natural hydrophobicity of polystyrene and PDMS enable component-substrate interactions via the hydrophobic force. The assembly fluid mixture was prepared by pipeting polystyrene microspheres into an ethanol–water mixture containing 8% water by volume. The components were dispersed in the fluid by shaking the mixture on a vortex mixing tool for a few minutes.

About 2 mL of the assembly fluid medium was pipetted into the assembly beaker, which is a second, smaller beaker suspended above the transducer and immersed 0.75 cm into water in the large beaker. The PDMS template was placed face-up in the beaker. A sufficient volume of the polystyrene component solution (between 300-400 μL, at a density of 2.26×10^9 components/mL) was added to the assembly beaker. A large oversupply of components, with more than 10^5 times as many microspheres as assembly sites on the template, was contained in this mixture volume. Power to the transducer was turned on after capping the small beaker, and the experiment was run undisturbed for 5 minutes. The template was then taken out of the assembly mixture, placed on a flat surface and allowed to air-dry for about a minute before examination with an inverted optical microscope.

The assembly yield was quantified by calculating the ratio of the number of wells of each size that were filled with components to the total number of wells of that size. After analysis, the components were detached from assembly sites on the template by placing the template at the bottom of the small beaker, adding a small volume (4 mL) of ethanol to
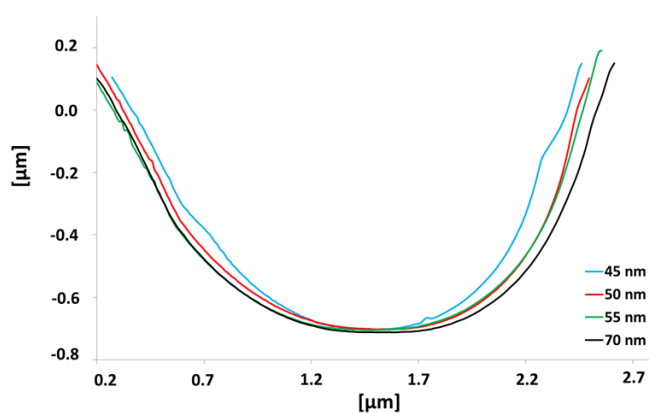
Fig 2: Atomic force microscopy (AFM) images of wells created in the deformable PDMS replica templates from master silica templates, etched from initial resist openings with nominal sizes of 45, 50, 55 and 70 nm.

the beaker, and placing the system in an ultrasonic bath for about 2 minutes. The template was then reused to ensure geometric consistency between runs. Experiments were also conducted previously under similar conditions for the self-assembly of polystyrene microspheres on the master silica template, as described in detail in [10]. Results obtained from these two sets of experiments were compared to assess the effect of the deformability of the template surface on assembly yield.

Results

The initial experiments were carried out using assembly templates in which the wells are nearly hemispherical and are well-matched to the components' diameters. The optical micrographs of Figure 3 show assembly as the voltage applied to the acoustic transducer (and hence its output power) is increased. The template in this case comprises an array of nominally uniformly-sized, nearly-hemispherical wells that were etched to a depth of approximately 1 μm from small (50 nm diameter) openings in the resist. At low values of transducer

voltage, low assembly yield is observed and most assembly sites are empty (Figure 3(A)). Low yield at low power is explained in [9]; at low enough levels of input power, the fluid forces cannot overcome the energy barriers at the edges of the wells to drive components into the assembly sites. Figure 3(B) shows the higher assembly yields that occur as voltage and input power are increased. The higher power enables the components to sample the sites, and components that match their wells' sizes begin to be trapped in the sites when the adhesive moments that promote component retention exceed the fluidic moments that promote component removal [7,8]. At an excitation voltage of about 50 V, the assembly yield rises to nearly 100%, as shown in Figure 3(C). At this stage, the retention effects dominate the removal effects. Any further increase in voltage strengthens the fluidic moments that promote component removal, and the yield starts decreasing.

The results of Figure 3 are similar to those observed with both rigid and deformable components assembled into rigid substrates [7-11], providing initial support for the success of assembly of deformable components into highly deformable substrates. However, the results of Figure 3 do not by themselves demonstrate that deformable templates cannot disrupt the assembly process. Successful assembly involves not only achieving high assembly yields for cases in which the components are well-matched to the wells, but also achieving low assembly yields when the components are poorly-matched to the wells. Since the template of Figure 3 contains nominally uniform, well-matched wells, it cannot demonstrate the ability to reject poorly-matched components.

Selectivity was demonstrated by characterizing assembly into wells that were etched from a range of different-sized openings in the e-beam resist; larger resist openings correspond to a larger final well diameter as well as larger deviations from the ideal hemispherical shape. Figure 4 plots the assembly yields that were measured for wells etched from resist openings ranging from 45 nm in diameter (the "nominal hole size") to 70 nm in diameter (25 nm larger than the nominal hole size) with a transducer voltage of 50 V. The assembly yield of polystyrene microspheres onto PDMS has its maximum values for wells that are 0-5 nm larger than the nominal size and begins to decrease for even slightly larger well sizes. The higher yield is obtained for wells etched from smaller resist openings since
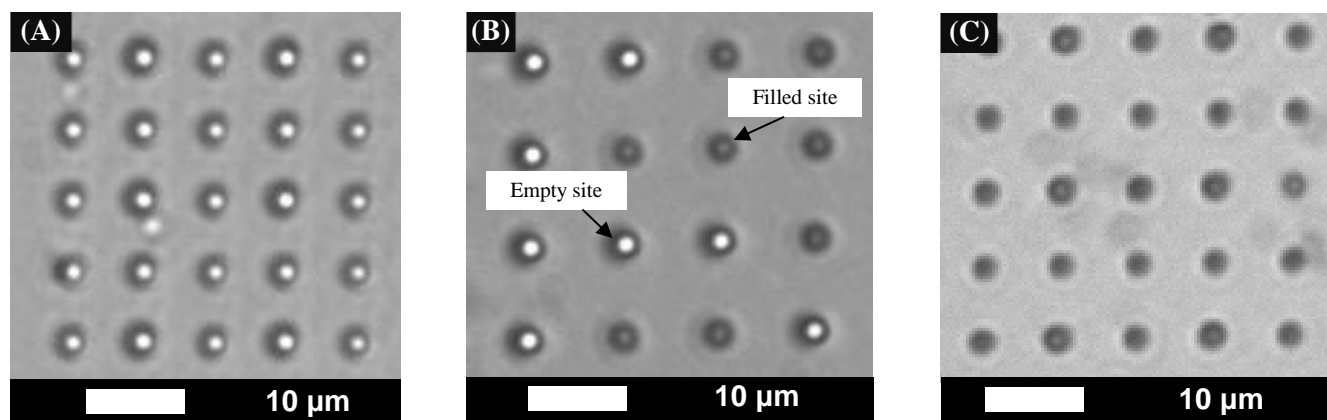
Fig. 3: Optical micrographs showing progressive stages of assembly in the TASR process upon increasing voltage on the acoustic transducer. (A) shows a portion of the TASR template assembled at 20V, with most wells observed to be empty as shown by their white centers. (B) shows an assembly template upon increasing the voltage to 30V. The increasing number of filled wells are identifiable by their dark centers. (C) shows the same region of the template after assembly at the optimum voltage of 50V, with all wells successfully filled with well-matched microspheres.
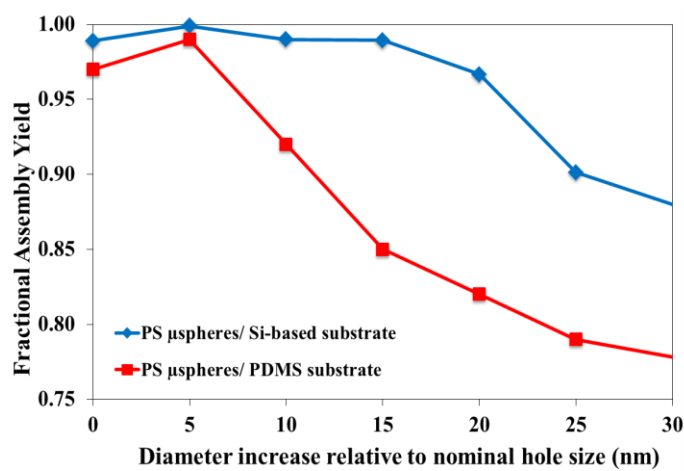
Fig. 4: Plot of measured fractional assembly yield versus the difference between the assembly site diameter and the nominal assembly site diameter. The nominal diameter is the diameter of a well etched from an initial resist opening of 45 nm on the master silicon template. Red squares describe assembly of polystyrene onto PDMS, and blue diamonds describe assembly of polystyrene onto the silicon-based master.

they match the components better in shape and size, as compared with wells created from larger resist openings. The significance of the observed results is confirmed by multiple measurements of yield in nominally identical experiments (50 V and 8% water fraction with polystyrene components). The variation in yield for those assembly conditions was less than 7%.

The successful size-selectivity of the assembly onto PDMS confirms that even extreme elastomer deformability does not prevent selective assembly and supports the principle that it is the onset of plastic deformation rather than purely elastic deformation that is of concern in this powerful type of shape-matched assembly. Selective assembly is successful despite a much larger contact area for the case of assembly onto the much more deformable PDMS template as compared with assembly onto the rigid template. The nominal contact area (i.e. the contact area without taking into account surface roughness) was calculated for 2 µm PS spheres assembling into ideal hemispherical wells of various dimensions under the influence of a typical 4 nN force. The calculations take into account the shrinkage of PDMS upon curing. For assembly into wells with 2.045 µm diameter (the nominal 2 µm size plus the size of the original resist opening), the contact areas are 1.2 µm^2 and 4.1 x 10^{-3} µm^2 for assembly onto PDMS and onto the more rigid material, respectively. For assembly into wells with 2.070 µm diameter (similar to the largest wells patterned from a 70 nm resist opening), the contact areas for PDMS and the more rigid material are 0.87 µm^2 and 3.1 x 10^{-3} µm^2, respectively. The contact area within a hemispherical well on the PDMS template is therefore approximately 290X larger (for the smallest wells) and 280X larger (for the largest wells) than the contact area within a well on the more rigid template. The contact areas will decline as the well size is increased and as the well deviates from an ideal hemispherical shape, but PDMS's larger contact area as compared with rigid substrates will be maintained. The results are also consistent with the model's predictions that the components and substrate will remain outside the plastic regime for the materials considered here.
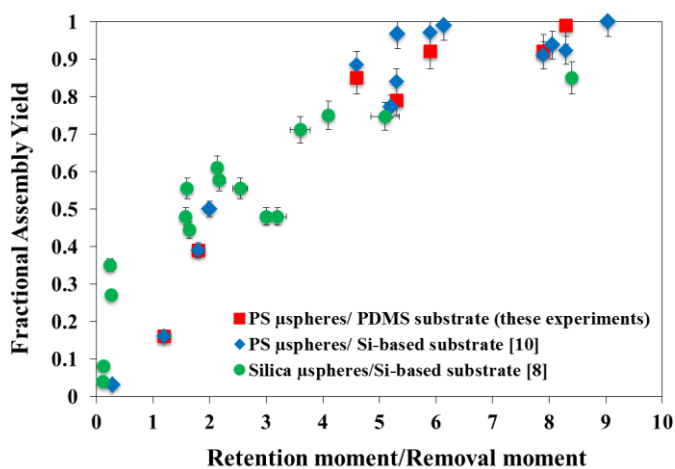
Fig. 5: Plot of measured fractional assembly yield versus ratio of moment promoting component retention to moment promoting component removal for deformable polystyrene components on deformable PDMS (the present data), deformable polystyrene components on rigid silicon-based substrates [10], and rigid silicon components on rigid silicon-based substrates [8]. The results shown here represent a range of experimental conditions, including different well diameters, assembly fluid compositions, and acoustic transducer voltages. The data fall onto a single curve.

The best way to demonstrate that elastic template deformation does not notably impact TASR-based size-selective assembly is to show that assembly into PDMS templates follows the same trend as assembly into the master silicon-based templates, to within the limits of the experiments. To compare assembly into the two templates, the data of Figure 4 are compared with the data from [10], in which similarly-sized (2.077 +/- 0.045 µm) components are assembled into the silicon-based template used here as a master pattern for the PDMS molding. The data from [10] are plotted for comparison in Figure 4. It is evident that the two curves are not identical. Although both sets of experiments are similar and show a high yield for wells etched from small resist openings, the yield for assembly onto PDMS declines somewhat more quickly than the yield for assembly into Si. For larger well sizes, the offset between the two curves is approximately 15 nm.

It is important to ask whether the offset between the two curves represents a meaningful difference between the two experiments (e.g. the slightly different geometries of the two experiments or a fundamental difference between assembly onto PDMS and assembly onto a rigid substrate) or a random variation that reflects experimental uncertainty. The different geometries include both sphere sizes and well sizes. The microspheres assembled onto the PDMS template have an average diameter that is approximately 73 nm smaller than the average diameter of the microspheres that were assembled onto the silicon-based master template. However, the effective difference in sizes is much less than 73 nm, for three reasons. First, the well-known shrinkage of PDMS during curing will result in the wells being smaller on the replicated template than on the silicon-based master. Assuming shrinkage of approximately 1% as reported in [33], the double PDMS molding process will create wells that are about 2% smaller than those of the master template. Since attack of the resist/oxide interface by the BOE results in imperfectly hemispherical wells, the wells may be characterized either by

their depth (i.e. approximately 2 μm in diameter) or by their width (i.e. approximately 2.5 μm in diameter), corresponding to a well shrinkage of between 40 nm and 50 nm. The smaller well size partially compensates for the smaller sphere size used for experiments on assembly onto PDMS. Second, the remaining effective size difference of 23 to 33 nm is less than the 80 nm and 45 nm standard deviations of the spheres' size distributions. Finally, the imperfectly hemispherical wells are characterized by a range of values for radius of curvature rather than by a single radius, further increasing the geometric uncertainty and the range of possibilities for successful assembly. The approximately 15 nm offset between the two curves observed in the experiments is well within the range of experimental size uncertainty. Figure 4 therefore shows that assembly onto PDMS and assembly onto rigid substrates are comparable to within the size resolution of the experiments.

Finally, the ratio of the adhesive moments that promote component retention to the fluidic moments that promote component removal were calculated for all of the experiments carried out here. The calculations were carried out using the original TASR model that was created to describe assembly of rigid components onto rigid templates [7-9]. Figure 5 plots the measured assembly yield vs. the calculated moment ratio for the present experiments. Also plotted for comparison are the corresponding curves for silica spheres assembled on the master templates and for polystyrene spheres assembled on the master templates as reported in [8,10]. To within the limits of the experimental uncertainties (e.g. the values of template roughness, fluidic forces, and acoustic excitations), the three cases fall along a single curve. These results confirm that, to within the limits of the model described above, assembly of deformable objects on PDMS substrates can be predicted with the same tools that are used for rigid systems, and that selective assembly can be successful.

Conclusions

These results demonstrate the successful application of a powerful size-selective assembly technique to the assembly of deformable components onto low-cost, replicated PDMS templates, greatly expanding the practical utility of the assembly technique. Because polystyrene is more easily plastically deformed than other polymers of interest, and because PDMS's deformability is very large, the present successful assembly constitutes a robust validation of the technique. Quantitative analysis of the results demonstrates that not only is the assembly successful, but it also proceeds in the same manner as assembly of rigid and deformable components onto more expensive, rigid master templates. Together with models that describe other aspects of the TASR process, the theoretical model presented here offers a tool to predict the circumstances under which a given set of material parameters will be consistent with TASR-based selective assembly. The model is validated by the successful assembly of plastically-deformable polystyrene components onto elastomeric PDMS substrates. Finally, the model's predictions that this process will be successful even for the assembly of cells onto common biopolymers such as PGS suggests that TASR can be a successful tool for biological applications such as structuring engineered tissues.

Acknowledgements

Notes and references

[a] Gunjan Agarwal is a Postdoctoral Associate in Microsystems Technology Laboratories (MTL) at the Massachusetts Institute of Technology, Cambridge, MA 02139, USA. Ph: 617-253-1465; E-mail: agarwalg@mit.edu

[b] Amelia Servi is a Graduate Research Assistant in the Department of Mechanical Engineering at the Massachusetts Institute of Technology, Cambridge, MA 02139, USA. Ph: 617-538-9125; E-mail: aservi@mit.edu

[c] Carol Livermore is an Associate Professor in the Department of Mechanical and Industrial Engineering at Northeastern University, Boston, MA 02115, USA. Ph: 617-373-4922; E-mail: livermore@neu.edu

1   Becker H, Gärtner C., Polymer microfabrication technologies for microfluidic systems, *Anal Bioanal Chem.*, 2008, 390(1):89-111.

2   O. Rötting, W. Röpke, H. Becker, C. Gärtner, Polymer microfabrication technologies, *Microsystem Technologies*, March 2002, Volume 8, Issue 1, pp 32-36.

3   Bettinger, C. J., Weinberg, E. J., Kulig, K. M., Vacanti, J. P., Wang, Y., Borenstein, J. T. and Langer, R., Three-Dimensional Microfluidic Tissue-Engineering Scaffolds Using a Flexible Biodegradable Polymer, *Adv. Mater.*, 2006, 18: 165–169.

4   Rossier, J., Reymond, F. and Michel, P. E., Polymer microfluidic chips for electrochemical and biochemical analyses, *Electrophoresis*, 2002, 23: 858–867.

5   Aaron S Goldstein, Tiffany M Juarez, Christopher D Helmke, Michael C Gustin, Antonios G Mikos, Effect of convection on osteoblastic cell growth and function in biodegradable polymer foam scaffolds, *Biomaterials*, Volume 22, Issue 11, June 2001, 1279-1288.

6   Jakab, K., Norotte, C., Marga, F., Murphy, K., Vunjak-Novakovic, G., & Forgacs, G. (2010), Tissue engineering by self-assembly and bio-printing of living cells, *Biofabrication*, 2(2), 022001.

7   S. Jung and C. Livermore, Achieving Selective Assembly with Template Topography and Ultrasonically Induced Fluid Forces, *Nanoletters*, Vol 5, no.11, p. 2188-94, 2005.

8   F. Eid, S. Jung, C. Livermore, Templated assembly by selective removal: simultaneous, selective assembly and model verification, *Nanotechnology* 19 (2008) 285602.

9   S. Jung, F. Eid, and C. Livermore, Modeling and Characterizing Initial Component Assembly in Templated Assembly by Selective Removal (TASR), submitted to *IEEE Transactions on Nanotechnology*.

10   G. Agarwal, A. Servi, F. Eid, and C. Livermore, Selective Self-Assembly of Polymer Structures using Templated Assembly by Selective Removal, *IEEE Transactions on Nanotechnology*, vol.10, no.3, pp.617-625, May 2011.

11 G. Agarwal, and C. Livermore, Chip-Based Size-Selective Sorting of Biological Cells using High Frequency Acoustic Excitation, *Lab on a Chip*, April 2011.

12 Samuel K. Sia and George M. Whitesides, Microfluidic devices fabricated in poly(dimethylsiloxane) for biological studies, *Electrophoresis* 2003, *24,* 3563–3576.

13 Ut-Binh T. Giang, Michael R. King, Lisa A. DeLouise, Microfabrication of Bubbular Cavities in PDMS for Cell Sorting and Microcell Culture Applications, *Journal of Bionic Engineering*, 5 (2008) 308–316.

14 Melikhan Tanyeri, Mikhil Ranka, Natawan Sittipolkul and Charles M. Schroeder, A microfluidic-based hydrodynamic trap: design and implementation, *Lab Chip*, 2011,11, 1786-1794.

15 Lukas Bogunovic , Ralf Eichhorn , Jan Regtmeier , Dario Anselmetti and Peter Reimann , Particle sorting by a structured microfluidic ratchet device with tunable selectivity: theory and experiment, *Soft Matter*, 2012,8, 3900-3907.

16 Javier L. Baylon-Cardiel , Nadia M. Jesús-Pérez , Ana V. Chávez-Santoscoy and Blanca H. Lapizco-Encinas, Controlled microparticle manipulation employing low frequency alternating electric fields in an array of insulators, *Lab Chip*, 2010,10, 3235-3242.

17 Jason G. Kralj, Michael T. W. Lis, Martin A. Schmidt and Klavs F. Jensen, Continuous Dielectrophoretic Size-Based Particle Sorting, *Analytical Chemistry*, 2006 78 (14), 5019-5025.

18 Lewpiriyawong, N., Yang, C. and Lam, Y. C., Continuous sorting and separation of microparticles by size using AC dielectrophoresis in a PDMS microfluidic device with 3-D conducting PDMS composite electrodes., *Electrophoresis*, 2010, 31: 2622–2631.

19 Ying Huang, Karla L. Ewalt, Marcus Tirado, Robert Haigis, Anita Forster, Donald Ackley, Michael J. Heller, James P. O'Connell, and Michael Krihak, Electric Manipulation of Bioparticles and Macromolecules on Microfabricated Electrodes, *Anaytical Chemistry*, 2001, 73, 1549-1559.

20 Justin E. Molloy and Miles J. Padgett. Lights, action: optical tweezers, *Contemporary Physics*, 2002, 43, 241-258.

21 Ching-Yu Chang, Yasufumi Takahashi, Tatsuya Murata, Hitoshi Shiku, Hsien-Chang Chang and Tomokazu Matsue, Entrapment and measurement of a biologically functionalized microbead with a microwell electrode, *Lab Chip*, 2009,9,1185-1192.

22 Theresia EB Stradal and Giorgio Scita, Protein complexes regulating Arp2/3-mediated actin assembly, *Current Opinion in Cell Biology*, Volume 18, Issue 1, February 2006, Pages 4-10.

23 Kum Cheong Tang, Julien Reboud, Yuan Li Kwok, Shu Ling Peng and Levent Yobas, Lateral patch-clamping in a standard 1536-well microplate format, *Lab Chip*, 2010, 10, 1044-1050.

24 Shannon L. Faley, Mhairi Copland, Donald Wlodkowic, Walter Kolch, Kevin T. Seale, John P. Wikswo and Jonathan M. Cooper, Microfluidic single cell arrays to interrogate signalling dynamics of individual, patient-derived hematopoietic stem cells, *Lab Chip*, 2009, 9, 2659-2664.

25 Chen, Qian, Sung Chul Bae, and Steve Granick, Directed self-assembly of a colloidal kagome lattice, *Nature* 469.7330 (2011): 381-384.

26 Khalil, Karim S., Amanda Sagastegui, Yu Li, Mukarram A. Tahir, Joshua ES Socolar, Benjamin J. Wiley, and Benjamin B. Yellen, Binary colloidal structures assembled through Ising interactions, *Nature communications* 3 (2012): 794.

27 Xia, Yunsheng, Trung Dac Nguyen, Ming Yang, Byeongdu Lee, Aaron Santos, Paul Podsiadlo, Zhiyong Tang, Sharon C. Glotzer, and Nicholas A. Kotov, Self-assembly of self-limiting monodisperse supraparticles from polydisperse nanoparticles, *Nature nanotechnology* 6, no. 9 (2011): 580-587.

28 Mesarovic, S. D., and Fleck, N. A., Frictionless Indentation of Dissimilar Elastic-Plastic Spheres, *Int. J. Solids Struct.*, 2000, 37, pp. 7071–7091.

29 W.R.Chang, I. Etsion and D. B. Bogy, An Elastic-Plastic Model for the Contact of Rough Surfaces, *ASME J. Tribol.*, 1987, 109, pp. 257 – 263.

30 Chang, W. R., Etsion, I., and Bogy, D. B., 1988, Static Friction Coefficient Model for Metallic Rough Surfaces, *ASME J. Tribol.*, 110, pp. 57–63.

31 T. Koerner, L. Brown, R. Xie and R. D. Oleschuk, Epoxy resins as stamps for hot embossing of microstructures and microfluidic channels Sensors and Actuators B, 2005, 1076, 32–639.

32 M. P. P. Briones, T. Honda, Y. Yamaguchi, M. Miyazaki, H. Nakamura and H. Maeda, A practical method for rapid microchannel fabrication in polydimethylsiloxane by replica molding without using silicon photoresi, J. Chem. Eng. Jpn., 2006, 39, 1108–1114.

33 Kyung M. Choi and John A. Rogers, A Photocurable Poly(dimethylsiloxane) Chemistry Designed for Soft Lithographic Molding and Printing in the Nanometer Regime, *Journal of the American Chemical Society*, 2003, *125* (14), 4060-4061.